SCANNING ELECTRON MICROSCOPY, NON-DISPERSIVE X-RAY ANALYSIS AND ELECTRON MICROPROBE STUDIES OF LUNAR SOIL, ROCKS AND MICROBRECCIA

J.L. Carter
Principal Investigator

The University of Texas at Dallas
P. O. Box 30365
Dallas, Texas 75230
(A/C 214) 231-1471

Progress Report

28 September 1972

Sponsored by

National Aeronautics and Space Administration
Grant No.: NGR 44-004-116, Suppl. # 1

The attached reprint (1), page-proofs (2), two preprints (3,4) and two abstracts (5,6) cover the areas of research completed and some of those that are in progress. Scanning electron microscopic studies of Apollo 15 and 16, and Luna 20 samples are in progress. Features similar to those seen on the previous Apollo materials were observed. As with the previous materials, microcraters have been found predominately on the dark brown glasses. A three-dimensional structural analysis of breccia 14318 is in progress. 27X photomosaics of two of the eight polished thin sections have been completed. Photomosaics of the glass surface of rock 15015,36 (3) and of the surface of several fragments from various Apollo 11, 15, 16 and Luna 20 samples have been made. Detailed analysis of the surfaces of the fragments are in progress.

No hypervelocity-type craters were observed at magnifications up to 11,500X on the glass surface of rock 15015,36 (3,5) suggesting that this surface was exposed neither to bombardment by micrometeroids nor to relatively high velocity projectiles in an impact-generated debris cloud. The surface of the glass has an assortment of non-silicate mound types (3,5). Detailed study of the mounds suggests a large portion of the metallic iron resulted from reduction of the molten silicate surface, whereas the sulfur was supplied mainly from an external source such as an impact-generated vapor cloud.

Chemical analyses of mineral fragments from four soil samples are in progress. A comparison of pyroxenes from soil samples 15501,53 and 15411,46 (4,6) reveals that thorough mixing of soil components has not occurred throughout the Apollo 15 sampling area, and that limitations must be applied to models involving mixing mechanisms and soil transport over long distances on the lunar surface.

The pyroxene population of soil sample 66081,5 amounts to only 2 to 3 percent of the total number of grains observed. The chemical analyses show them to be bronzites and diopsidic augites, present in a ratio of 5:2, respectively. Plots of the Ti/Al relationship (atoms per formula unit) reveal close groupings about either the Ti:Al = 1:2 line or the Ti:Al = 1:4 line, with less scatter than observed for the pyroxenes from Apollo 15 soils (4). The most magnesium-rich orthopyroxenes cluster about the Ti:Al =1:4 line. Olivines are as abundant as pyroxenes and preliminary data suggest compositions of Fa_{10}-Fa_{37}. These mineral compositions, which are reminiscent of those derived from ultramafic and mafic rocks that have undergone little fractionation, suggest that they are from a different rock type than the abundant anorthosites that appear to be the source of the majority of the samples obtained from the Apollo 16 sampling sites.

Attachments

1) Carter, J.L. (1972). "Morphology and chemical composition of metallic mounds produced by H_2 and C reduction of material of simulated lunar composition", Lunar Sci.-III (C. Watkins, ed.), 125-127.

2) Carter, J.L. and D.S. McKay (1972). "Metallic mounds produced by reduction of material of simulated lunar composition and implications on the origin of metallic mounds on lunar glasses", Proc. Third Lunar Sci. Conf., Geochim. Cosmochim. Acta, Suppl. 3, 1, M.I.T. Press.

3) Carter, J.L. (1972). "Morphology and chemistry of glass surface of breccia 15015,36", Proc. Fourth Lunar Sci. Conf.

4) Taylor, H.C. Jim and J.L. Carter (1972). "Chemistry of pyroxenes from Apollo soil 15501,53", Proc. Fourth Lunar Sci. Conf.

5) Carter, J.L. (1972). "Surface morphology and chemistry of rocks 15015,36", Trans. A.G.U. (abstract).

6) Taylor, H.C. Jim and J.L. Carter (1972). "A comparison of pyroxenes from lunar soil sample 15411,46 and 15501,53", Trans. A.G.U. (abstract).

P. 125

MORPHOLOGY AND CHEMICAL COMPOSITION OF METALLIC MOUNDS PRODUCED BY H_2 AND C REDUCTION OF MATERIAL OF SIMULATED LUNAR COMPOSITION. James L. Carter, University of Texas at Dallas, Geosciences Division, Dallas, Texas 75230.

A joint project was initiated with David S. McKay at NASA/MSC, Houston to test the possibility of producing by reduction processes complex metallic iron and iron sulfide mounds which are similar to those observed by numerous workers on the surface of lunar glass particles (e.g., Agrell, et al. 1970; Carter and MacGregor, 1970; McKay, et al. 1970; Carter, 1971). A glass of composition similar to dark brown lunar glass was made from reagent grade chemicals.

The preliminary experiment involved placing approximately one gram of ground glass with various amounts of sulfur in weight percent (0.0, 0.24, 0.49, 1.0) in carbon crucibles and placing them in a glow bar furnace with an argon atmosphere at 1450° C for five minutes, quenching in air and storing the resulting glass sphere in a plastic vial. Other samples were placed in alumina boats in a glow bar furnace for three minutes at 1450° C and flushed with argon, then a gas consisting of 5% H_2, 95% argon was flowed over the samples for two minutes. One sample was reduced with the hydrogen mixture for fifteen minutes.

Preliminary results of the scanning electron microscope and electron microprobe examinations are shown in Table 1. The complex iron sulfide and metallic iron mounds formed by reduction with hydrogen are generally layered (cross section shown schematically in Fig. 1). The outer layer is iron sulfide or a mixture of iron sulfide and metallic iron, the interior is metallic iron and the mound material next to the silicate host is iron sulfide. Sometimes the mounds are multilayered. Sometimes the complex mounds have a thin waist of iron sulfide. Similar waists of iron sulfide around metallic iron mounds have been seen on lunar glasses (Agrell, et al 1970; Carter, 1971). Dimples are sometimes present. The silicate surface of the dimple is covered by dendritic sheafs of iron sulfide and isolated metallic iron mounds. In some complex mounds spherules of silicate material are present. In one example, one to five micron in diameter spherules occur on the surface of an ameboid-shaped group of metallic iron and iron sulfide mounds. The spherules consist of a particle of what appears to be aluminum oxide which is surrounded by silicate material and in turn the margin of the spherule is surrounded by iron sulfide. No metallic mounds with inclusions of silicate spherules have been recognized on lunar glasses.

The complex iron sulfide and metallic iron mounds formed by reduction with carbon are generally layered (cross section shown schematically in Fig. 2). The interior of a mound is a mixture of iron sulfide and metallic iron. The outer layer of pure metallic iron is generally discontinuous. The surface of the mound next to the silicate host is iron sulfide. The mounds commonly have a waist of metallic iron. No complex iron sulfide and metallic iron mounds on lunar silicate spherules have been recognized with waists of metallic iron. There is a void beneath a mound. The silicate surface of the void is

p. 126
covered with mounds or stringers of iron sulfide.

These data suggest that 1) the ratio of sulfur to iron is of fundamental importance to the morphological nature of metallic mounds, 2) the growth time is important to the morphological nature of metallic mounds, and 3) most metallic mounds on lunar glass spheres did not form by reducing processes in situ. However, during the melting of lunar soil such as during a major meteoritic event hydrogen, as a result of trapped solar winds in the lunar soil, may play at least a secondary role in the formation of metallic iron and may be responsible in part for the formation of metallic iron mounds with waists of iron sulfide.

Table 1. Description of mounds.

Reducing Agent	Wt. % S	Description of mounds
H_2	0.0	Mounds occur as irregular stringers or web-like metallic iron objects with crinkled surfaces. Others are flat, porous, fan-shaped metallic iron objects up to 20 microns in longest dimension. A fifteen minute run resulted in a massive network of connected circular metallic iron mounds with crinkled surfaces.
C	0.0	Numerous individual metallic iron mounds occur up to 50 microns in diameter which are surrounded by smaller metallic iron mounds.
H_2	0.24	Mounds occur as trains of connected metallic iron octahedra. Also irregularly shaped ameboid-like complex metallic iron and iron sulfide mounds occur.
C	0.24	Numerous individual mounds occur up to 100 microns in diameter. Some of the larger mounds are surrounded by masses of coalesced small metallic iron mounds. Some mounds are complex mixtures of iron sulfide and metallic iron; others are porous, dendritic, iron sulfide. Dimples with an inner dimple are common. The silicate surface of the inner dimple is covered with iron sulfide mounds.
H_2	0.49	Individual complex iron sulfide and metallic iron mounds occur up to 200 microns in diameter. Trains of connecting circular metallic iron mounds (2-15 microns in diameter) with rough surfaces are present also. The larger mounds in the trains have six-sided flat-topped metallic iron objects on their surface. The metallic iron trains grade into areas of dendritic metallic iron mounds. Occasionally ameboid-shape complex iron sulfide and metallic iron mounds up to 300 microns in longest dimension are seen. Shrinkage cracks around their margins are poorly developed. Dimples are common. Some dimples have isolated circular metallic iron mounds and irregular dendritic areas of iron sulfide on their surface. One to five microns in diameter spherules occur on the surface of some of the ameboid-shape mounds. The spherules consist of a particle of what appears to be aluminum oxide which is surrounded by silicate material and in turn the margin of the spherule is sur-

P.127

rounded by iron sulfide.

C 0.49 Numerous mounds occur up to 150 microns in diameter. Some of the larger mounds are surrounded by masses of coalesced small metallic iron mounds. The mounds consist of metallic iron that is surrounded by a mixture of iron sulfide and metallic iron. Metallic iron margins are common. Dimples with an inner dimple are common. The silicate surface of the inner dimple is covered with mounds and stringers of iron sulfide.

H_2 1.0 Individual mounds occur up to 300 microns in diameter and are complex mixtures of dendritic iron sulfide and metallic iron. Some mounds 10-50 microns in diameter have a patchy layer of metallic iron over a core consisting of a mixture of iron sulfide and metallic iron. Some mounds have a thin waist of iron sulfide. The larger mounds have well developed cooling cracks around their margins. Some larger mounds contain spherules of silicate material. Dimples are common. The upper margin of the dimple is textured and has dendritic areas of iron sulfide on its surface. Individual octahedra of metallic iron approximately five microns in diameter occur.

C 1.0 Numerous complex individual mounds of metallic iron and iron sulfide occur up to 200 microns in diameter and are sometimes surrounded by masses of coalesced small metallic iron mounds. Individual mounds have metallic iron margins. Dimples with an inner dimple are common. The silicate surface of the inner dimple is covered with iron sulfide mounds.

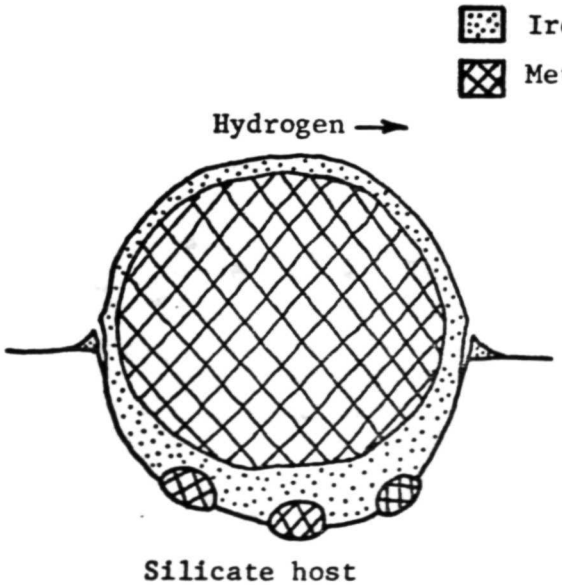

Fig. 1. Schematic cross section of complex mound formed by reduction with hydrogen.

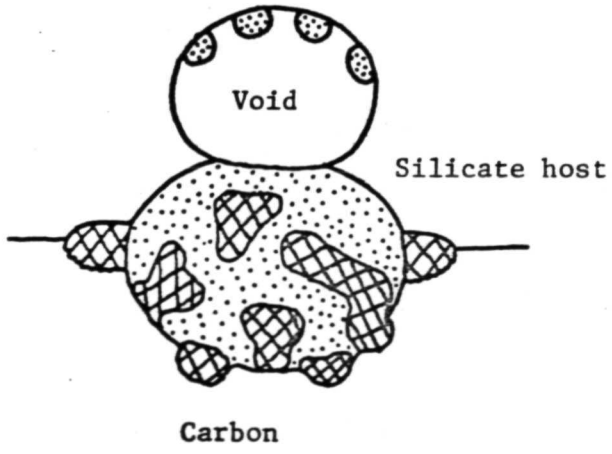

Fig. 2. Schematic cross section of complex mound formed by reduction with carbon.

Proceedings of the Third Lunar Science Conference
(Supplement 3, *Geochimica et Cosmochimica Acta*)
Vol. 1, pp. 0000–0000
The M.I.T. Press, 1972

Metallic mounds produced by reduction of material of simulated lunar composition and implications on the origin of metallic mounds on lunar glasses*

JAMES L. CARTER

University of Texas at Dallas, Geosciences Division, Division of Earth and Planetary Sciences, P.O. Box 30365, Dallas, Texas 75230

DAVID S. MCKAY

National Aeronautics and Space Administration, Manned Spacecraft Center, Houston, Texas 77058

Abstract—Silicate glass of composition similar to brown lunar glass was reduced with carbon and hydrogen. The typical complex iron sulfide and metallic iron mound formed by reduction with carbon is zoned. Its interior is metallic iron or a mixture of iron sulfide and metallic iron. The outer layer is pure metallic iron which is generally discontinuous, but the surface of the mound next to the silicate host is iron sulfide. This type of mound commonly has a waist of metallic iron and a void beneath it. The silicate surface of the void is covered with droplets or stringers of iron sulfide.

The complex iron sulfide and metallic iron mounds formed by reduction with hydrogen generally are zoned. The outer layer is iron sulfide or a mixture of iron sulfide and metallic iron, but the interior is metallic iron and iron sulfide, and the mound material next to the silicate host is iron sulfide. On the surface of some complex mounds, globules of silicate material are present. In one example, the globules consist of particles of aluminum oxide surrounded by silicate material. In turn, the margin of the globules is surrounded by iron sulfide. Dimples are present and the surface of the dimples is covered by dendritic sheaths of iron sulfide and isolated metallic iron globules.

These data suggest that: (1) the ratio of sulfur to iron has direct bearing on the morphology of metallic mounds; (2) the growth time also influences the nature of metallic mounds; and (3) mounds produced by reduction with carbon are different from mounds produced by reduction with hydrogen.

The laboratory data suggest that most metallic mounds on lunar glasses did not form by reducing processes *in situ*. However, during the melting of lunar soil, for example during a meteoroid impact event, hydrogen and to a lesser extent carbon, as a result of trapped solar winds, may play at least a secondary role in the formation of metallic iron, and may be responsible in a large part for the formation of mounds that are low in nickel which commonly occur in trains or patterns on the glass-bonded agglutinates. In addition, it is inferred from these data that the iron mounds rich in nickel, cobalt, sulfur, and phosphorus may be remobilized components of meteorites and probably formed in the impact-generated debris cloud.

INTRODUCTION

SEVERAL DISTINCT morphological and chemical types of metallic mounds occur on lunar glass spheres and irregularly shaped glasses: (1) FeS (McKay *et al.*, 1970; Carter and McGregor, 1970); (2) metallic Fe (Ramdohr and El Goresy, 1970; Agrell *et al.*, 1970; Carter and MacGregor, 1970); (3) mixtures of metallic Fe and FeS (McKay *et al.*, 1970; Carter and McGregor, 1970); (4) metallic Fe and Ni (Agrell *et al.*, 1970; Carter and MacGregor, 1970; Frondel *et al.*, 1970; McKay *et al.*, 1970); (5) mixtures of Fe, Ni, and P (Carter and MacGregor, 1970; Goldstein *et al.*, 1970;

* Contribution No. 210, Geosciences Division, University of Texas at Dallas, P.O. Box 30365, Dallas, Texas 75230.

Carter, 1971); (6) mixtures of Fe, Ni, P, S, and C (Carter and MacGregor, 1970); (7) Fe and Ni with waists of FeS (Duke *et al.*, 1970; Agrell *et al.*, 1970; Frondel *et al.*, 1970; Goldstein *et al.*, 1970; Carter, 1971). In addition, as many as five magnetic phases may be present within glass spheres (Adler *et al.*, 1970; Agrell *et al.*, 1970; Duke *et al.*, 1970; McKay *et al.*, 1970; Ramdohr and El Goresy, 1970; Simpson and Bowie, 1970; Winchell and Skinner, 1970; Griscom and Marquardt, 1972; Wosinski *et al.*, 1972).

The iron sulfide mounds occur mainly on glass-bonded agglutinates and dust-welded glass spheres (McKay *et al.*, 1970; Carter and MacGregor, 1970). Trains of metallic iron mounds occur on glass-bonded agglutinates and irregularly shaped glassy objects (Ramdohr and El Goresy, 1970; Carter and MacGregor, 1970; Carter, 1971). The complex masses of iron sulfide and metallic iron, or iron sulfide and metallic iron-nickel occur as distinct mounds on glass spheres and irregularly shaped glassy objects (Ramdohr and El Goresy, 1970; Carter and MacGregor, 1970; Carter. Some metallic iron-nickel mounds are surrounded by waists of iron sulfide. The iron, nickel, and phosphorus mounds occur as individual mounds, groups of mounds or complex amoeboid-shaped mounds (Carter and MacGregor, 1970; Goldstein *et al.*, 1970; Carter, 1971). The iron, nickel, phosphorus, sulfur, and carbon mounds occur as complex masses on irregularly shaped glass fragments (Carter and MacGregor, 1970).

The origin of the various types of mounds on silicate surfaces has not been clearly established. There are at least three possible origins for the mounds: (1) reduction of silicate *in situ*; (2) splashes; and (3) vapor deposition and subsequent growth of mounds. The source of the material forming mounds of the latter two categories may be (1) reduction of iron-bearing material (both lunar and meteoritic), (2) remelted components of meteoritic material, or (3) remelted components of lunar material.

In order to better understand the possible origins of the various types of mounds, a survey project was initiated at NASA/MSC, Houston, to test the possibility of producing complex metallic iron and iron sulfide mounds similar to those observed on the surfaces of lunar glass particles by reduction processes *in situ*. A glass of composition similar to dark brown lunar glass was made from reagent grade chemicals. (Table 1). The glass was ground in a tungsten-carbide mixer-mill for five minutes. Various amounts of elemental sulfur were added to aliquots of this homogenized ground glass.

The preliminary experiment involved placing approximately one gram of ground glass with various amounts of sulfur in carbon crucibles, heating them in a glo-bar furnace with an argon atmosphere at 1450°C for five minutes, and quenching the totally liquid silicate globule in air to form a glass spheroid approximately 9 mm by 7 mm. There was approximately 60 mm^2 of liquid silicate surface in contact with the carbon crucible. Other samples were placed in alumina boats in a glo-bar furnace for three minutes at 1450°C and flushed with argon; subsequently, a gas consisting of 5% hydrogen and 95% argon at one atmosphere was flowed over the samples for two minutes. One sample was reduced with the hydrogen mixture for fifteen minutes. The surface of the liquid silicate available for reduction by hydrogen was approximately four times greater than in the carbon experiment.

Table 1. Chemical composition in weight percent of simulated brown lunar glass*

SiO_2	40.37
Al_2O_3	14.49
Cr_2O_3†	0.3
TiO_2	7.50
FeO	15.36
MgO	8.13
MnO†	0.2
CaO	13.25
Na_2O	0.59
K_2O	0.03
P_2O_5	0.03
S	0.05
TOTAL	100.30

* X-ray fluorescence analysis by J. M. Rhodes.
† Added to glass but not analyzed for by x-ray fluorescence.

Experimental Results

Results of scanning electron microscope and electron microprobe examinations are shown in Table 2. A JEOLCO JSM-1 scanning electron microscope and an ARL EMX-SM electron microprobe was used in the examinations. A wide variety of mounds and dimples or voids were observed on the glass surface (Table 2; Fig. 1). In addition, metallic iron globules up to 4 μ in diameter occur to a depth of approximately 300 μ into both the glass spheroid and the glass produced in the hydrogen reduction experiment. In this 300 μ zone of reduction, the iron content of the glass in the carbon-reduced samples is 9% to 11% less than in the starting material, and in the hydrogen-reduced samples it is 11% to 12% less than in the starting material.

Mounds

The sulfur content of the glass influences the composition and morphology of the mound. In general, mounds formed from samples rich in sulfur contain more iron sulfide and are larger than mounds formed from low sulfur samples (Table 2).

Reduction with carbon. When the glass with no sulfur added was reduced by contact with carbon, simple iron mounds were formed which display either a finely convoluted surface texture (Fig. 2) or, in some cases, a pattern of triangular-shaped ridges (Figs. 3 and 4). The finely convoluted structure may be iron oxide formed during quenching of the liquid silicate spheroid in air. A similar convoluted structure was seen on some lunar metallic mounds (Carter and MacGregor, 1970).

More complex zoned metallic iron and iron sulfide mounds are formed when sulfur was added to the glass (Table 2; Figs. 1, 5 to 12). The interior zone or core of the mound is predominantly metallic iron (Fig. 5) or a mixture of metallic iron and iron sulfide (Figs. 6 and 7). The outer zone consists of a discontinuous coating of metallic iron on the free surface (Figs. 5, 6, 8, 9, 11, and 12) and a waist of metallic iron surrounds the mound at the contact of the free surface of the mound with the silicate glass host in some specimens (Figs. 8 to 10). The underside of the mound in contact with glass lacks the metallic iron coating and is iron sulfide (Table 2; Figs. 5

Table 2. Description of mounds

Reducing agent	Wt. % S	Description of mounds
C	0.0	Numerous individual metallic iron mounds occur up to 50 μ in diameter, which are surrounded by smaller metallic iron mounds.
H_2	0.0	Mounds occur as irregular stringers or web-like metallic iron objects with crinkled surfaces. Others are flat, porous, fan-shaped metallic iron objects up to 20 μ in longest dimension. A fifteen-minute run resulted in a massive network of connected circular metallic iron mounds with crinkled surfaces.
C	0.24	Numerous individual mounds occur up to 100 μ in diameter. Some of the larger mounds are surrounded by masses of coalesced small metallic iron mounds. Some mounds are complex mixtures of iron sulfide and metallic iron; others are porous, dendritic, iron sulfide. Dimples with an inner dimple are common. The silicate surface of the inner dimple is covered with iron sulfide mounds.
H_2	0.24	Mounds occur as trains of connected metallic iron octahedra. Irregularly shaped, amoeboid-like, complex metallic iron, and iron sulfide mounds also occur.
C	0.49	Numerous mounds occur up to 150 μ in diameter. Some of the larger mounds are surrounded by masses of coalesced small metallic iron mounds. The mounds consist of metallic iron that is surrounded by a mixture of iron sulfide and metallic iron. Metallic iron margins are common. Dimples with an inner dimple are common. The silicate surface of the inner dimple is covered with mounds and stringers of iron sulfide.
H_2	0.49	Individual complex iron sulfide and metallic iron mounds occur up to 200 μ in diameter. Trains of connecting circular metallic iron mounds (2 to 15 μ in diameter) with rough surfaces are present also. The larger mounds in the trains have six-sided, flat-topped metallic iron objects on their surface. The metallic iron trains grade into areas of dendritic metallic iron mounds. Amoeboid-shape complex iron sulfide and metallic iron mounds up to 300 μ in longest dimension rarely are seen. Shrinkage cracks around their margins are poorly developed. Dimples are common. Some dimples have isolated circular metallic iron mounds and irregular dendritic areas of iron sulfide on their surface. One to five micron diameter spherules occur on the surface of some of the amoeboid-shape mounds. The spherules consist of a particle that appears to be aluminum oxide, which is surrounded by silicate material, and in turn the margin of the spherule is surrounded by iron sulfide.
C	1.0	Numerous complex individual mounds of metallic iron and iron sulfide occur up to 200 μ in diameter and are sometimes surrounded by masses of coalesced small metallic iron mounds. Individual mounds have metallic iron margins. Dimples with an inner dimple are common. The silicate surface of the inner dimple is covered with iron sulfide mounds.
H_2	1.0	Individual mounds occur up to 300 μ in diameter and are complex mixtures of dendritic iron sulfide and metallic iron. Some mounds 10 to 50 μ in diameter have a patchy layer of metallic iron over a core consisting of a mixture of iron sulfide and metallic iron. Some mounds have a thin waist of iron sulfide. The larger mounds have well-developed cooling cracks around their margins. Some larger mounds contain spherules of silicate material. Dimples are common. The upper margin of the dimple is textured and has dendritic areas of iron sulfide on its surface. Individual octahedra of metallic iron approximately 5 μ in diameter occur.

and 6). The presence of tungsten (approximately ≤ 56 wt. %) and cobalt (approximately ≤ 6 wt. %) in the mounds (Fig. 5) shows that the molten iron acts as a scavenger for these elements even though they occur in small amounts in the silicate host (W, 0.08 wt. %; Co, 0.017 wt. %, as determined by electron microprobe techniques). Lunar metallic iron contains relative high concentrations of tungsten (Wänke *et al.*, 1970).

Reduction with hydrogen. When the glass with no sulfur added is reduced by hydrogen, metallic iron is formed (Table 2; Figs. 13 to 16). The metallic iron may occur as a massive coating (Fig. 13) or as isolated spongy masses (Fig. 14), or more typically as interconnected amoeboid-like stringers and mounds (Figs. 15 and 16). These

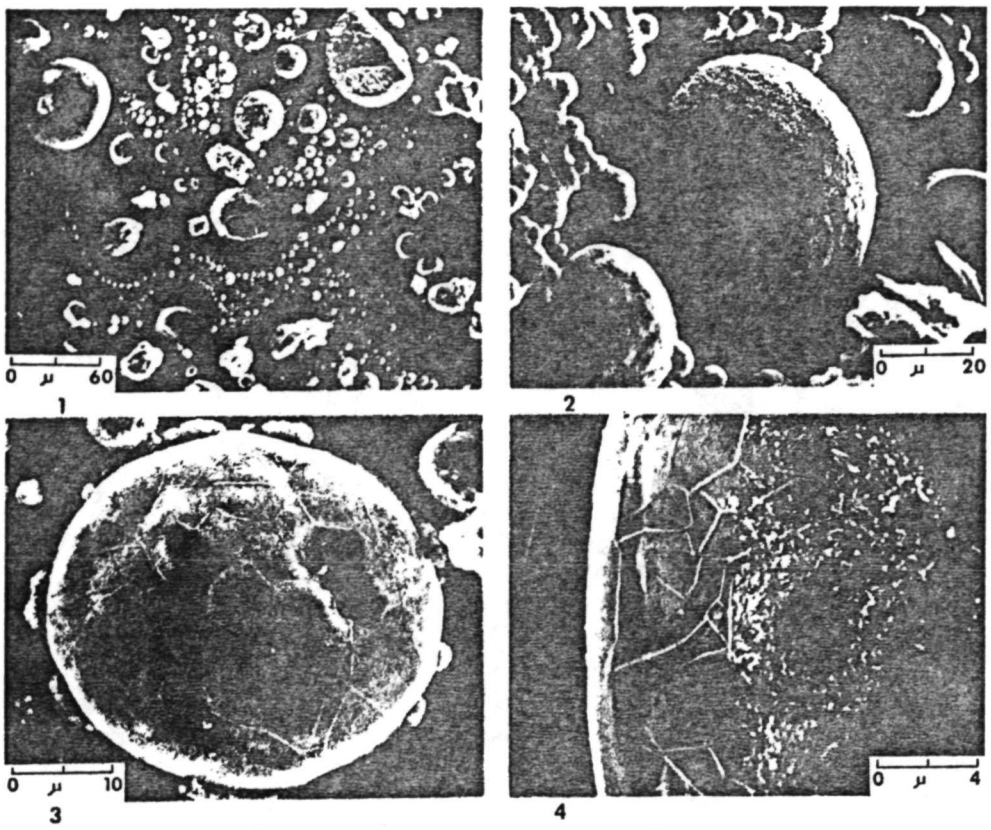

Fig. 1. View of part of a silicate surface (containing 0.23% sulfur) reduced by carbon showing dimples, individual mounds, and trains of mounds. The large dimple has an inner dimple (center of photograph) which was formed by trapped gas.

Fig. 2. Dominant type of metallic iron mound formed by carbon reduction on silicate host that contained 0.06% sulfur. The finely convoluted surface of the mounds is similar to certain mound surfaces observed in Apollo 11 material.

Fig. 3. Typical metallic iron mound on silicate surface (no sulfur present) that was reduced by carbon. Note pattern of interconnected triangular ridges on surface of mound.

Fig. 4. Enlarged view of interconnected triangular ridges on the surface of a metallic iron mound seen on a carbon-reduced silicate sphere that contained 0.06% sulfur.

mounds are usually zoned and contain a core of massive iron surrounded by a thin coating of convoluted iron (Fig. 16). The convoluted surface is similar to that observed with carbon reduction (Fig. 12) and may be iron oxide formed during quenching of the liquid silicate in air.

When sulfur is added to the glass, more complex zoned mounds are formed by hydrogen reduction (Table 2; Figs. 17 to 24). The interior zone may be either metallic iron or a mixture of metallic iron and iron sulfide (Table 2; Fig. 17). Mixed iron sulfide cores are more common in mounds formed from glasses with higher sulfur contents (Table 2). This core is covered by a mixture of iron sulfide and metallic iron on the free

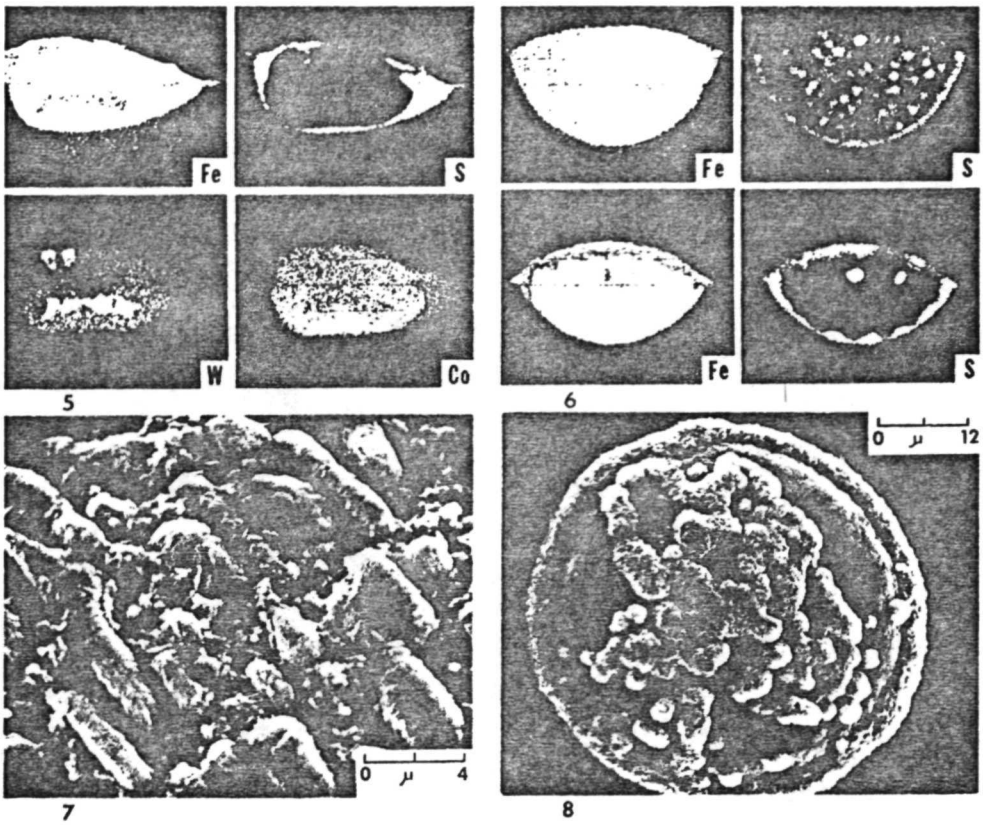

Fig. 5. X-ray intensity maps showing distribution of Fe. S. W. and Co in cross section of mound produced by carbon reduction of silicate containing 0.49% S. Scale is 15 μ per division.

Fig. 6. X-ray intensity maps showing distribution of Fe and S in cross section of two mounds produced by carbon reduction of silicate containing 0.49% S. Scale in upper section is 15 μ per division and 10 μ per division in the lower section.

Fig. 7. Upside-down enlarged view of largest mound in upper right portion of Fig. 1. Large metallic iron masses are seen in a fine-grained iron sulfide matrix.

Fig. 8. Complex metallic mound on silicate surface (containing 0.16% sulfur) that was reduced with carbon. The waist is metallic iron, while the central mass is iron sulfide that is blanketed by a mixture of iron sulfide and metallic iron.

surface (Figs. 17 to 19) and by pure iron sulfide in the area next to the glass host (Table 2; Fig. 17). In some cases, a thin waist of iron sulfide is present at the contact between the free surface of the mounds and the glass host (Figs. 20 to 22).

In addition to isolated well-developed mounds (Figs. 20 and 21), interconnecting and partially coalesced amoeboid-like masses may develop (Figs. 23 to 26). Some of the individual mounds and coalesced mounds display a poorly developed octahedral form (Fig. 26). On Fig. 26, tiny isolated mounds are reduced in size and abundance

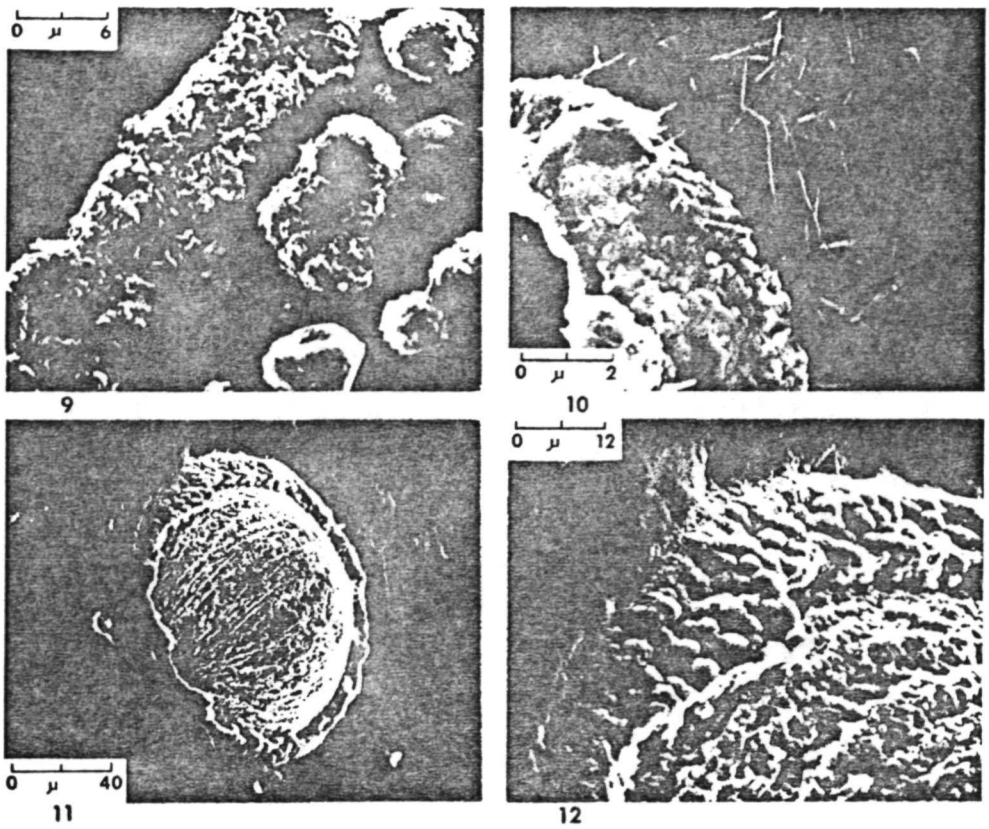

Fig. 9. Enlarged view of the margin of a typical complex metallic mound on silicate surface (containing 0.49% sulfur) that was reduced with carbon. Note the finely crinkled surface on the metallic iron margin.

Fig. 10. Enlarged view of a portion of the carbon reduced silicate surface (containing 1% sulfur) adjacent to a metallic iron mound. Needles of metallic iron and spherules of metallic iron (0.1 μ in diameter) formed on the silicate surface.

Fig. 11. Complex mound on silicate surface (containing 0.24% sulfur) that was reduced with carbon. The outer metallic iron and iron sulfide layer was partially stripped away during quenching, revealing an interior of dendritic iron.

Fig. 12. Enlarged view of upper left margin of mound in Fig. 11 showing details of the outer metallic iron and iron sulfide layer and the dendritic iron core. The outer layer consists of interlocking spherules in contrast to the dendritic structure of the iron core.

in the vicinity of larger partially coalesced mounds, suggesting that the larger mounds were being supplied with iron and sulfur from the surrounding area during growth.

Silicate spherules

Some complex mounds contain silicate spherules within the mounds and protruding from their surfaces (Table 2).

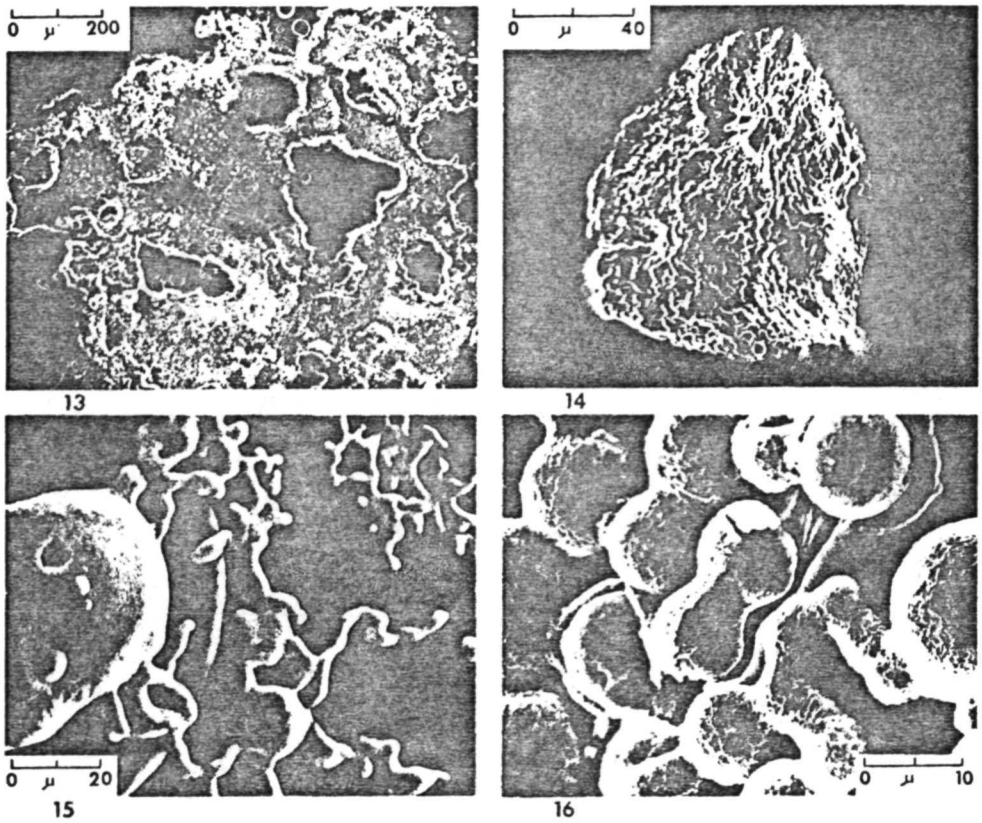

Fig. 13. Typical silicate surface reduced by hydrogen with no sulfur present; the surface is massive metallic iron.

Fig. 14. Isolated fan-shaped area of spongy metallic iron on silicate surface reduced by hydrogen (no sulfur present). Spherules of silicate material are present in the lower right portion of the fan-shaped object.

Fig. 15. Interconnected amoeboid-like masses of metallic iron on silicate surface (no sulfur present) that was reduced by hydrogen. Note globules of silicate material on surface of the largest iron mass in the left center of the photograph.

Fig. 16. Enlarged view of interconnected metallic iron spherules formed on silicate surface (no sulfur present) that was reduced by hydrogen for fifteen minutes. Note layered nature of the mounds and the finely convoluted surface on the outer layer.

Reduction with carbon. A very small fraction of the mounds contain silicate spherules protruding from their surfaces (Figs. 27 and 28). This glass is of similar composition to the host glass and it may be simply silicate material trapped in the mound during formation and growth. No mound on lunar samples has been observed with spherules of silicate material on its surface.

Reduction with hydrogen. Many of the larger amoeboid-like masses produced when larger amounts of sulfur are present contain silicate spherules on their surfaces (Table 2; Figs. 14, 15, 23, 24, 29, and 30). The globules on the surfaces of metallic

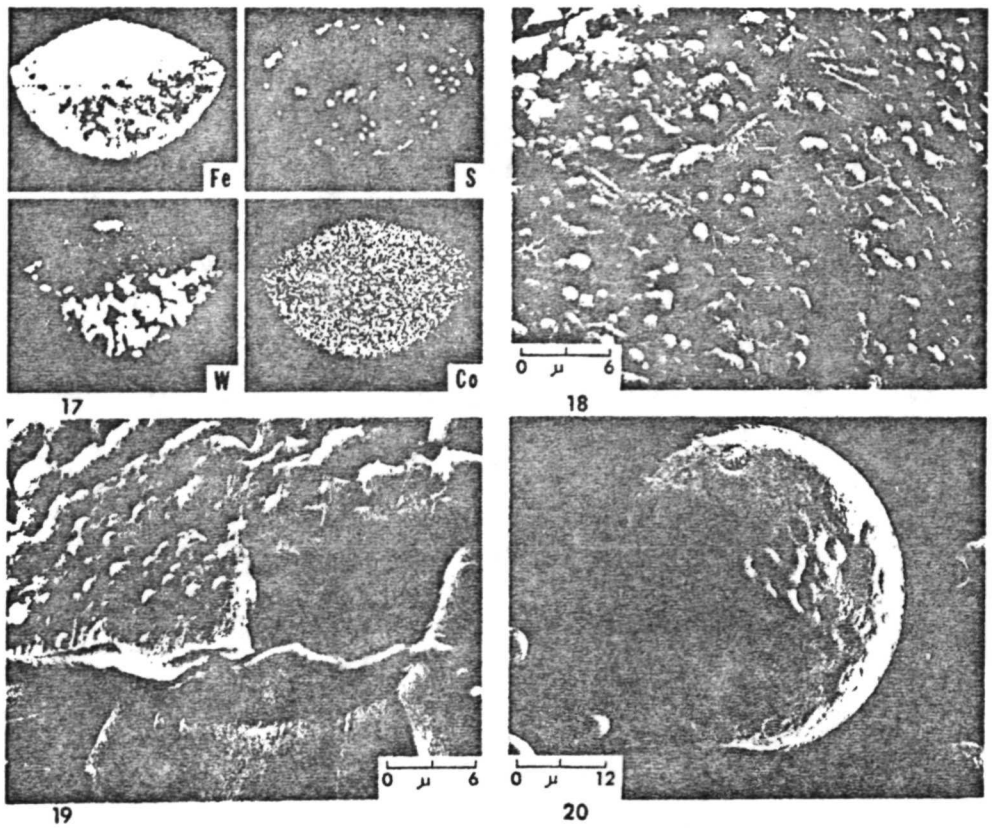

Fig. 17. X-ray intensity maps showing distribution of Fe. S, W, and Co in cross section of mound produced by hydrogen reduction of silicate containing 0.49% S. Grid is 20 μ per division.

Fig. 18. Enlarged view of the surface of a complex metallic mound formed on a silicate surface (containing 1% sulfur) that was reduced by hydrogen. Globules of iron sulfide are embedded in the finely convoluted surface of the same composition.

Fig. 19. Enlarged view of the surface of a complex metallic mound formed on a silicate surface (containing 1% sulfur) that was reduced by hydrogen. The iron sulfide skin was broken during quenching revealing an interior of interlocking metallic iron crystals.

Fig. 20. Isolated mound with waist of iron sulfide on silicate surface (containing 1% sulfur) that was reduced by hydrogen. The textured circular patches are iron sulfide suggesting that the mound has an incomplete coating of metallic iron.

mounds shown in Figs. 14 and 15 are silicate in composition and, like those seen on metallic mounds produced by reduction with carbon, appear to be simply silicate material trapped in the mounds during formation and growth. However, the silicate globules on the central massive metallic body in Fig. 18 apparently are different. An enlarged view of a silicate globule is shown in Fig. 29. The spherules less than 0.5 μ in diameter on the surface of the silicate globule are metallic iron. The composition of the silicate globules is similar to the host silicate, but there are areas that are

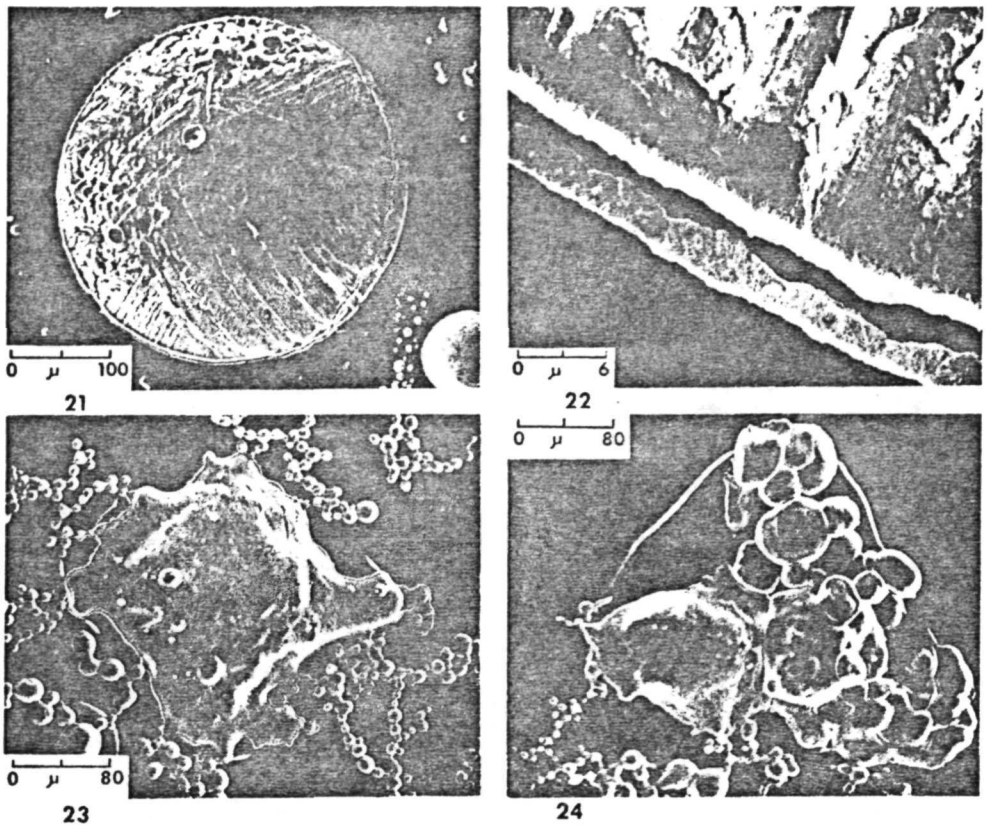

Fig. 21. Large complex mound on silicate surface (containing 1 % sulfur) that was reduced by hydrogen. Iron sulfide skin covers dendritic sheaths of metallic iron. Dark globules of silicate material can be seen on surface of the mound.

Fig. 22. Enlarged view of the lower left portion of Fig. 21 showing a waist of iron sulfide. Note the well-developed cooling crack around the margin of the mound.

Fig. 23. Complex amoeboid-like mass of metallic iron and iron sulfide on silicate surface (containing 0.49 % sulfur) that was reduced by hydrogen. The globules on the amoeboid-like mass are composed of silicate material. Note the trains of interconnected metallic iron mounds.

Fig. 24. Complex mass of metallic iron and iron sulfide mounds on silicate surface (containing 0.49 % sulfur) that was reduced by hydrogen. Silicate material forms globules on the large center left mass.

enriched in alumina suggesting that the silicate spherules are not simply incorporated molten droplets of the silicate host, but may be condensates. This latter view is supported by the nature of the silicate droplets shown in Fig. 19 and enlarged in Fig. 30. The globules that are 1 to 5 μ in diameter are silicate in composition. The globules consist of a particle of what appears to be aluminum oxide surrounded by silicate material. In turn, the margin of the silicate globules is surrounded by iron sulfide.

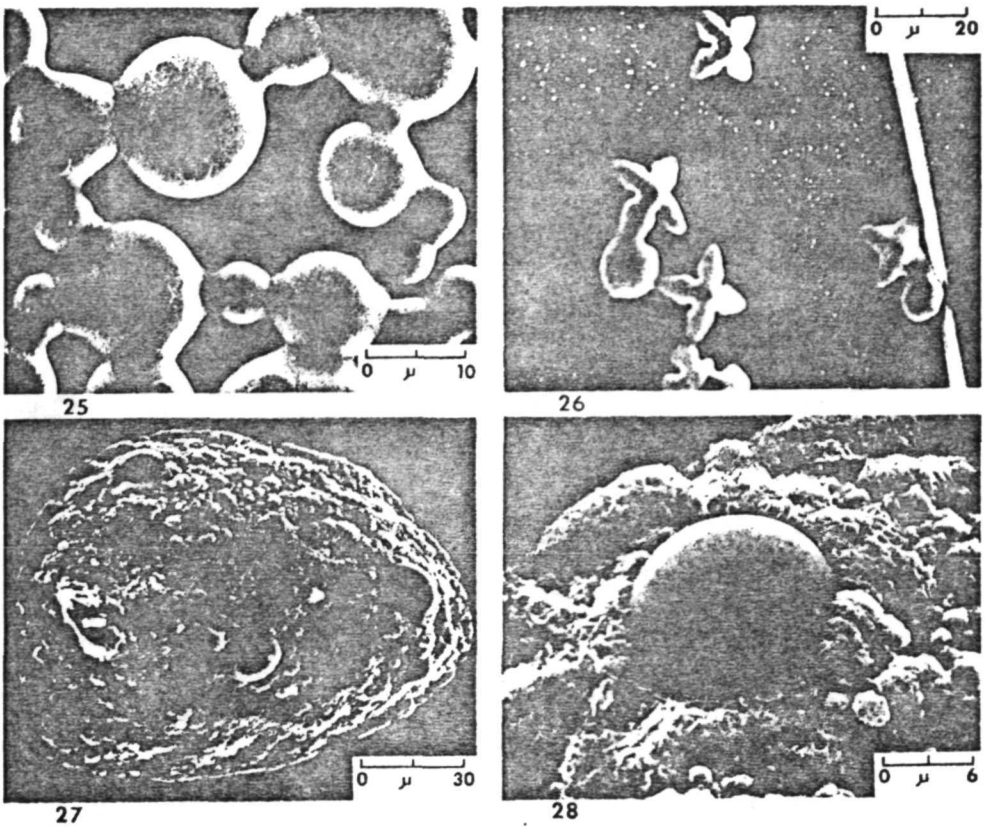

Fig. 25. Enlarged view of the trains of interconnected metallic iron mounds on a different area of the surface shown in Fig. 23. Note the pseudohexagonal platelets of metallic iron on the spherules; some platelets are twinned.

Fig. 26. Metallic iron octahedra on silicate surface (containing 1% sulfur) that was reduced by hydrogen. Note the small size and lower concentration of metallic iron mounds near the octahedra.

Fig. 27. Rare metallic iron mound containing spherules of silicate material formed during carbon reduction on silicate surface that contained 0.16% sulfur.

Fig. 28. Enlarged view of the upper left portion of Fig. 27 showing silicate spherule surrounded by metallic iron.

Dimples and voids

Some of the mounds were lost from the glass surface during quenching, leaving depressions or dimples (Table 2; Figs. 1, 31 to 34, and 37 to 40).

Reduction with carbon. The dimples of carbon-reduced samples sometimes contain an interior depression or void formed before the mound was removed (Figs. 31 and 32). This void probably was gas filled. The material formed on the surface of the void is metallic iron if no sulfur has been added to the glass (Fig. 31), whereas very small iron sulfide mounds commonly are present on the surface of these voids (Fig. 32) and

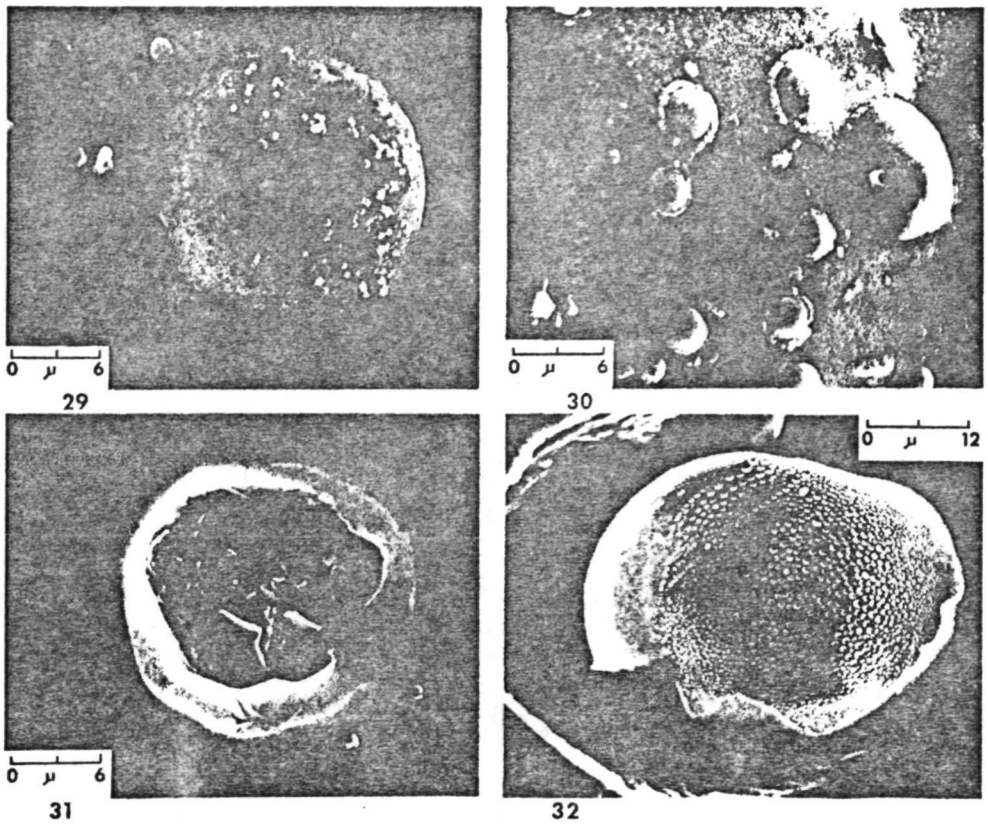

Fig. 29. Enlarged view of the silicate globule in center left of the amoeboid-like mass shown in Fig. 23; metallic iron spherules can be seen on its surface.

Fig. 30. Enlarged view of the left center portion of Fig. 24 showing silicate spherules that are surrounded by waists of iron sulfide. Note the triangular-shaped inclusion of apparently aluminum oxide in the largest silicate globule.

Fig. 31. Dimple in a silicate surface (no sulfur present) that was reduced by carbon. Note that the surface of the inner dimple contains blades of metallic iron.

Fig. 32. Dimple in a silicate surface (containing 0.24% sulfur) that was reduced by carbon. The surface of the dimple is covered with sheaths of iron sulfide, while the inner dimple is covered with globules of iron sulfide that are arranged in geometrical patterns.

on the surface of the silicate host which was in contact with the mound (Figs. 32 to 34) if sulfur has been added to the glass. Very similar dimples containing central voids are seen on some lunar glass surfaces (Fig. 35; also Carter and MacGregor, 1970, Figs. 28 and 33). However, they generally do not contain deposits on their surfaces (Fig. 36; also Carter and MacGregor, 1970).

Reduction with hydrogen. As with carbon reduction, dimples are formed when mounds are lost from the cooling silicate glass host. In both cases the loss of mounds is enhanced by differential contraction of the mound and the silicate host during

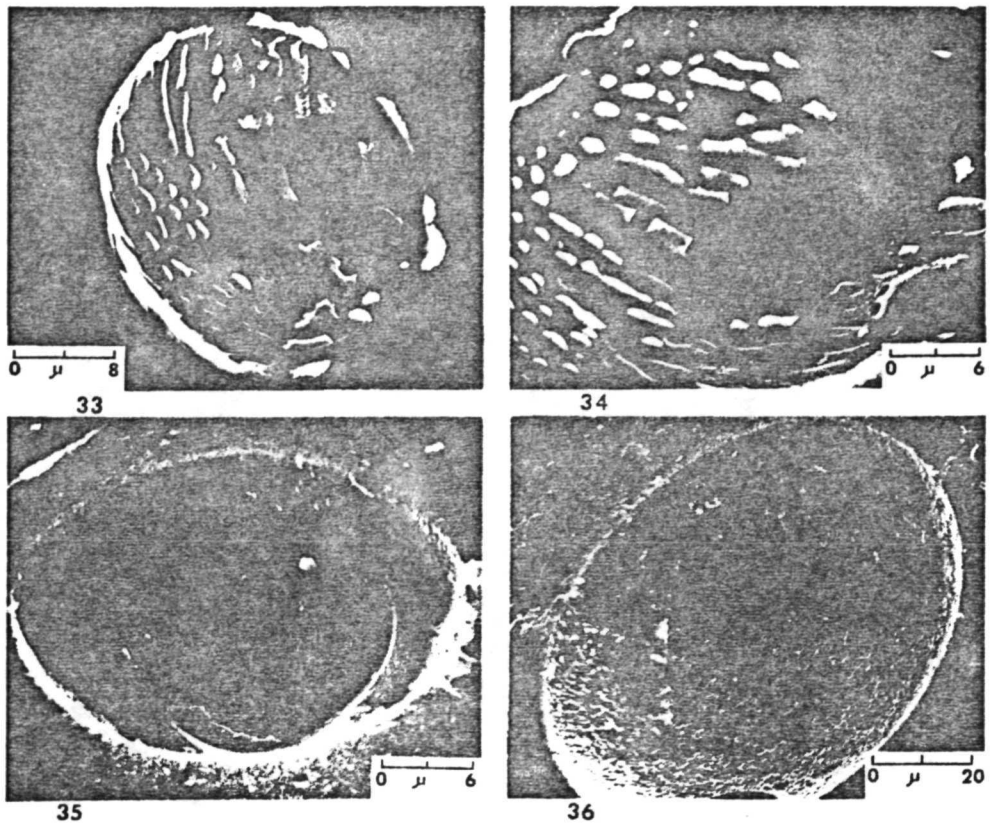

Fig. 33. Dimple in a silicate surface (containing 0.16% sulfur) that was reduced by carbon. Note that the surface of the dimple is covered with isolated globules and sheaths of iron sulfide.

Fig. 34. Enlarged view of the surface of a dimple seen in a silicate surface (containing 0.49% sulfur) that was reduced by carbon. The surface of the dimple is covered with isolated globules and sheaths of iron sulfide. Note the pattern on the dimple surface left by the loss of the iron sulfide.

Fig. 35. Dimple in an Apollo 11 brown silicate glass sphere. Note pattern of iron sulfide spherules on surface of inner dimple.

Fig. 36. Dimple in another Apollo 11 brown silicate glass sphere. Note pattern on surface of dimple.

cooling. This contraction may form a circumferential cooling crack (Figs. 21 and 22). Similar cooling cracks are present in lunar samples (Carter and MacGregor, 1970; McKay *et al.*, 1970; Carter, 1971).

Dimples formed by the loss of mounds on hydrogen-reduced glass display attached fragments of the dendritic iron sulfide mound and isolated globules of metallic iron (Figs. 35 to 38). Similar dimples are present on lunar glass spherules (Figs. 35 and 36; also Carter and MacGregor, 1970, Figs. 28, 31, 33 to 35, and 40).

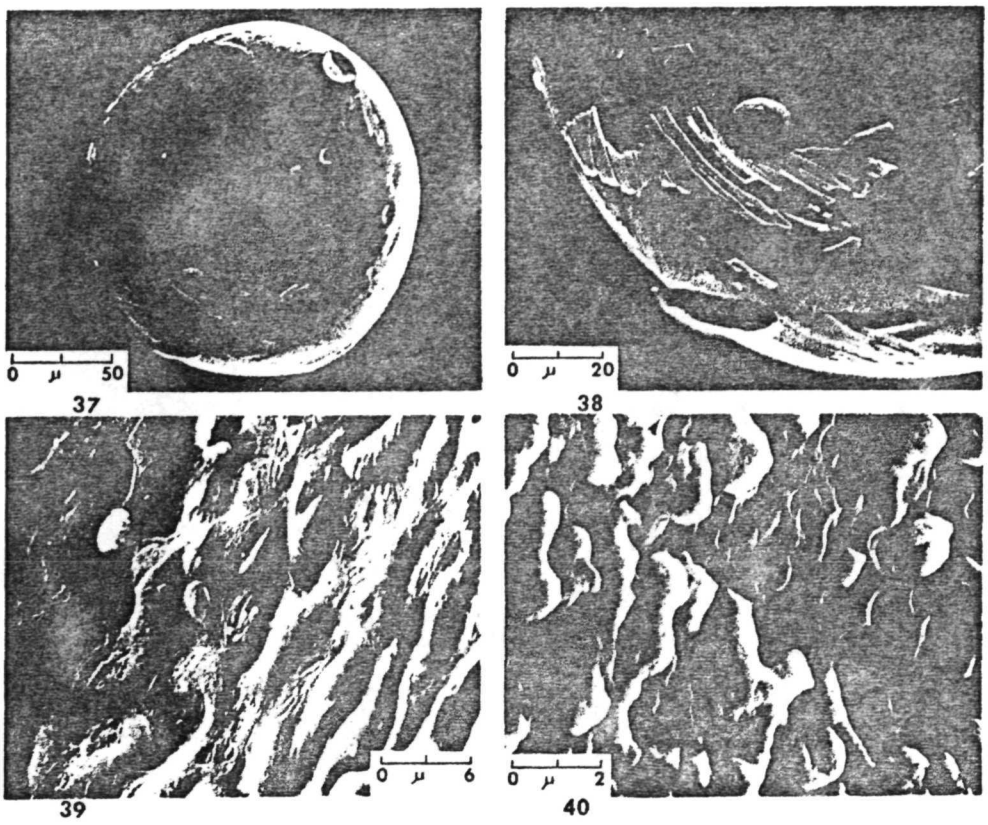

Fig. 37. Dimple in a silicate surface (containing 0.49 % sulfur) that was reduced by hydrogen. Globules on surface of dimple are metallic iron. Fragments of the dendritic iron sulfide mound are attached to the dimple surface.

Fig. 38. Enlarged view of the lower left portion of the dimple surface in Fig. 37. Note the metallic iron globule and the attached fragments of the dendritic iron sulfide mound.

Fig. 39. Enlarged view of a dimple surface in a silicate surface (containing 0.49 % sulfur) that was reduced by hydrogen showing a textured surface.

Fig. 40. Enlarged view of another dimple surface on silicate surface (containing 0.49 % sulfur) that was reduced by hydrogen. Note adhering masses of iron sulfide and impressions left by loss of iron sulfide.

Discussion and Conclusions

These data suggest that: (1) the ratio of sulfur to iron has a direct bearing on the morphology of metallic mounds; (2) the growth time also influences the nature of metallic mounds; and (3) mounds produced by reduction with carbon are different from mounds produced by reduction with hydrogen.

The typical mound formed by *in situ* reduction of sulfur-bearing silicate by contact

with carbon is a mass of metallic iron or a mixture of metallic iron and iron sulfide with an outer layer of metallic iron that commonly is discontinuous (Table 2; Figs. 5 to 9, 11, and 12). The mound commonly has a waist of metallic iron (Figs. 8 to 10). No complex metallic mounds with waists of metallic iron have been recognized on lunar glasses.

The typical isolated mound formed by *in situ* reduction of silicate material containing sulfur with hydrogen is a complex mixture of iron sulfide and metallic iron (Table 2; Fig. 17). The outer layer is a complex mixture of iron sulfide and metallic iron (Figs. 17 to 21), and the mound itself commonly is encircled with a thin waist of iron sulfide (Figs. 20 to 22). Waists of iron sulfide around metallic iron mounds rich in nickel have been reported on lunar glasses (Duke *et al.*, 1970; Agrell *et al.*, 1970; Frondel *et al.*, 1970; Goldstein *et al.*, 1970; Carter, 1971). Reduction with hydrogen of glass with no sulfur added produces metallic iron. This metallic iron may occur as a massive coating (Fig. 13), as isolated spongy masses (Fig. 14) or more typically as interconnected amoeboid-like stringers and mounds (Figs. 15 and 17). Interconnected amoeboid-like stringers and mounds are present on lunar glasses (Carter and MacGregor, 1970; McKay *et al.*, 1970; Carter, 1971).

The nature of the interface between the metallic mound and the silicate host is important to the understanding of the origin of a mound. Globules of iron sulfide characteristically cover the surfaces of dimples formed by reduction with carbon *in situ*, if sulfur is present in the silicate (Figs. 31 to 34). In contrast, the surfaces of dimples formed by reduction with hydrogen have imprints and fragments of dendritic iron sulfide sheaths and isolated metallic iron globules that comprised the mound (Figs. 37 to 40). A comparison of these dimples with the dimples seen on lunar glasses (Figs. 35 and 36; also Carter and MacGregor, 1970, Figs. 33 to 35; Carter, 1971, Figs. 7, 14 to 16, and 29) suggests that carbon was not a significant contributor to the formation of lunar metallic mounds, with the possible exception of the mound that left the imprint shown by Fig. 35, but that hydrogen may have contributed to the formation of lunar metallic mounds. The surface of the inner dimple in Fig. 35 has droplets of iron sulfide on it. The surface of all other inner dimples observed on lunar materials are smooth (Carter and MacGregor, 1970) suggesting that the voids under the mounds did not contain sulfur vapor.

The wide variation in mound morphology produced by reduction processes *in situ* (which includes the amoeboid-like mounds formed by reduction with hydrogen) suggests that some of the morphological types of mounds seen on lunar glasses could have formed by reduction processes *in situ* (e.g., those seen on the irregularly shaped glassy objects, Carter, 1971, Figs. 27 to 31). The most likely origin for the mounds that are rich in iron, nickel, cobalt, sulfur, and phosphorus is that they are remobilized components of meteorites (Goldstein and Yakowitz, 1971). The mounds that are rich in iron, nickel, cobalt, sulfur, phosphorus, and carbon probably also are remobilized components of meteorites with some possible addition of solar wind carbon (Holland *et al.*, 1972; Pillinger *et al.*, 1972).

From Figs. 5, 6, and 17, it is seen that isolated mounds formed by *in situ* reduction on the surface of molten silicate have unequal radii of curvature. The surface in contact with the silicate melt has the shortest radius of curvature. Lunar metallic

globules with unequal radii of curvatures are shown by Frondel *et al.* (1970, Fig. 12) and Mason *et al.* (1970, Figs. 2 and 3), and as suggested by Frondel *et al* (1970) they may have solidified as droplets on cooling silicate surfaces. Also of interest is the observation that the metallic iron acts as a scavenger incorporating the tungsten and cobalt from the tungsten carbide mixer mill (Figs. 5 and 17). This suggests that other siderophile elements may be incorporated in the iron metal during reduction of silicate materials containing those elements. Thus alloyed iron metal may form by *in situ* reduction processes on the lunar surface.

From these data it would appear that most metallic mounds on lunar glass spheres did not form by reduction processes *in situ* with the possible exception of the glass-bonded agglutinates, but formed as splashed, condensates or some origin not specified. Glass-bonded agglutinates are formed when impact-produced silicate liquid penetrates lunar soil. These agglutinates are typically vesicular and the release of implanted solar wind gases (primarily hydrogen and helium) from the heated soil particles may be the main vesicle-forming mechanisms (McKay and Ladle, 1971). This solar wind hydrogen, and to a lesser extent solar wind carbon, may play a major role in the formation of mounds low in nickel which often occur in trains or patterns on the glass-bonded agglutinates. Reduction processes, at least in part, may be responsible for the metallic iron present on the surface of some vesicles (Carter, 1971).

In addition to reduction by hydrogen and carbon, lunar samples heated by impact would be expected to show some reduction caused by loss of molecular oxygen at high temperatures. Gibson and Johnson (1971) and de Maria (1971) show evolution of molecular oxygen at temperatures of about 1400°C when lunar samples are heated in vacuum. However, Gibson and Johnson (1971) ascribed this oxygen evolution to the solution of iron into the platinum crucible. Gibson and Moore (1972) reported that oxygen does not evolve appreciably at temperatures up to 1400°C if an alumina crucible is used. At some higher temperature, however, metallic iron would be expected to form by the release of molecular oxygen from molten glass and iron globules within the glass and iron mounds on glass surfaces would be produced (Agrell *et al.*, 1970; Housley *et al.*, 1970). Metallic iron may be produced also by vacuum reduction of molten iron sulfide (Housley *et al.*, 1970).

A by-product of hydrogen reduction of iron-bearing silicate material is water [$FeO(glass) + H_2(gas) \rightarrow Fe(metal) + H_2O(gas)$]. This water, if produced in the hot ejecta blanket or base surge deposit of an impact (Pearce and Williams, 1972), may be retained in the deposit for a short time and thus may be the source of the water in the lunar "geothite" reported by Agrell *et al* (1972). Pearce and Williams (1972) produced metallic iron by reduction of the simulated brown lunar glass powder at temperatures of 800 to 1000°C, times between 5 hours and 74 hours, and oxygen fugacitites between 1 and 2 orders of magnitude below the IW buffer curve.

The conclusions are reached that: (1) complex metallic and sulfide mounds are produced from silicate glass of lunar composition by carbon or hydrogen reduction, (2) such mounds and the related dimples are similar in chemistry and morphology to some of those found on lunar silicate glass particles, and (3) reduction may be an important mechanism for the formation of some lunar complex metallic and sulfide mounds.

Acknowledgments--Supported by NASA Contract NAS 9-10221 and NASA Grant NGR-44-004-116 and NGL-44-004-001. We thank J. B. Toney for technical assistance and J. M. Rhodes, who performed the x-ray fluorescence analysis of the simulated brown lunar glass. Critical review by H. Axon, J. Goldstein, A. Hales, E. Padovani, D. Presnall, and H. Taylor has contributed to the improvement of the manuscript.

REFERENCES

Adler I. Walter L. S. Lowman P. D. Glass B. P. French B. M. Philpotts J. A. Heinrich K. J. F. and Goldstein J. I. (1970) Electron microprobe analysis of Apollo 11 lunar samples. *Proc. Apollo 11 Lunar Sci. Conf., Geochim. Cosmochim. Acta*, Suppl. 1, Vol. 1, pp. 87–92. Pergamon.

Agrell S. O. Scoon J. H. Muir I. D. Long J. V. P. McConnell J. D. C. and Peckett A. (1970) Observations on the chemistry, mineralogy and petrology of some Apollo 11 lunar samples. *Proc. Apollo 11 Lunar Sci. Conf., Geochim. Cosmochim. Acta*, Suppl. 1, Vol. 1, pp. 93–128. Pergamon.

Agrell S. O. Scoon J. H. Long J. V. P. and Coles J. N. (1972) The occurrence of goethite in a microbreccia from the Fra Mauro formation (abstract). In *Lunar Science—III* (editor C. Watkins), pp. 7–9, Lunar Science Institute Contr. No. 88.

Carter J. L. (1971) Chemistry and surface morphology of fragments from Apollo 12 soil. *Proc. Second Lunar Sci. Conf., Geochim. Cosmochim. Acta*, Suppl. 2, Vol. 1, pp. 873–892. M.I.T. Press.

Carter J. L. and MacGregor I. D. (1970) Mineralogy, petrology, and surface features of some Apollo 11 samples. *Proc. Apollo 11 Lunar Sci. Conf., Geochim. Cosmochim. Acta*, Suppl. 1, Vol. 1, pp. 247–275. Pergamon.

De Maria G., Balducci G., Guido M., and Piacente V. (1971) Mass spectrometric investigation of the vaporization process of Apollo 12 lunar samples. *Proc. Second Lunar Sci. Conf., Geochim. Cosmochim. Acta*, Suppl. 2, Vol. 2, pp. 1367–1380. M.I.T. Press.

Duke M. B. Woo C. C. Bird M. L. Sellers G. A. and Finkelman R. B. (1970) Lunar soil: size distribution and mineralogical constituents. *Science* **167** 648–650.

Frondel C. Klein C. Jr. Ito J. and Drake J. C. (1970) Mineralogical and chemical studies of Apollo 11 lunar fines and selected rocks. *Proc. Apollo 11 Lunar Sci. Conf., Geochim. Cosmochim. Acta*, Suppl. 1, Vol. 1, pp. 445–474. Pergamon.

Gibson E. K. Jr. and Johnson S. M. (1971) Thermal analysis-inorganic gas release studies of lunar samples. *Proc. Second Lunar Sci. Conf., Geochim. Cosmochim. Acta*, Suppl. 2, Vol. 2, pp. 1351–1366. M.I.T. Press.

Gibson E. K. Jr. and Moore G. W. (1972) Inorganic gas release and thermal analysis of Apollo 14 and 15 soils. *Proc. Third Lunar Sci. Conf., Geochim. Cosmochim. Acta*, Suppl. 3, Vol. **0**, pp. **0000–0000**. M.I.T. Press.

Goldstein J. I. Henderson E. P. and Yakowitz H. (1970) Investigation of lunar metal particles. *Proc. Apollo 11 Lunar Sci. Conf., Geochim. Cosmochim. Acta*, Suppl. 1, Vol. 1, pp. 499–512. Pergamon.

Goldstein J. I. and Yakowitz H. (1971) Metallic inclusions and metal particles in the Apollo 12 lunar soil. *Proc. Second Lunar Sci. Conf., Geochim. Cosmochim. Acta*, Suppl. 2, Vol. 1, pp. 177–191. M.I.T. Press.

Griscom D. L. and Marquardt C. L. (1972) Electron spin resonance studies of iron phases in lunar glasses and simulated lunar glasses (abstract). In *Lunar Science—III* (editor C. Watkins), pp. 341–343, Lunar Science Institute Contr. No. 88.

Holland P. T. Simoneit B. R. Wszolek P. C. McFadden W. H. and Burlingame A. L. (1972) Carbon chemistry of the lunar surface. *Nature* **235**, 252–253.

Housley R. M. Blander M. Abdel-Gawad M. Grant R. W. and Muir A. H. Jr. (1970) Mössbauer spectroscopy of Apollo 11 samples. *Proc. Apollo 11 Lunar Sci. Conf., Geochim. Cosmochim. Acta*, Suppl. 2, Vol. 2, pp. 1351–1366. Pergamon.

Housley R. M. Grant R. W. and Abdel-Gawad M. (1972) Study of excess Fe metal in the lunar fines by magnetic separation (abstract). In *Lunar Science—III* (editor C. Watkins), pp. 392–394, Lunar Science Institute Contr. No. 88.

McKay D. Morrison D. Lindsay J. and Ladle G. (1970) Origin of small lunar particles and breccia from the Apollo 11 site. *Proc. Apollo 11 Lunar Sci. Conf., Geochim. Cosmochim. Acta*, Suppl. 1, Vol. 1, pp. 673–694. Pergamon.

McKay D. S. and Ladle G. (1971) Scanning electron microscope study of particles in the lunar soil. In *Proc. 4th Annual Scanning Electron Microscope Symposium*, pp. 177–184. I.I.T. Research Inst., Chicago.

Mason B. Fredriksson K. Henderson E. P. Jarosewich E. Melson W. G. Towe K. M. and White J. S. Jr. (1970) Mineralogy and petrology of lunar samples. *Proc. Apollo 11 Lunar Sci. Conf., Geochim. Cosmochim. Acta*, Suppl. 1, Vol. 1, pp. 655-660. Pergamon.

Pearce G. W. and Williams R. J. (1972) Excess iron in lunar breccias and soils: possible origin (abstract). *Trans. Amer. Geophys. Union* **53**, No. 4, 360.

Pillinger C. T. Cadogan P. H. Eglinton G. Maxwell J. R. and Mays B. J. (1972) Simulation study of lunar carbon chemistry. *Nature Phys. Sci.* **235**, 108-109.

Ramdohr P. and El Goresy A. (1970) Opaque minerals of the lunar rocks and dust from Mare Tranquillitatis. *Science* **167**, 615-618.

Simpson P. R. and Bowie S. H. U. (1970) Quantitative optical and electron-probe studies of opaque phases in Apollo 11 samples. *Proc. Apollo 11 Lunar Sci. Conf., Geochim. Cosmochim. Acta*, Suppl. 1, Vol. 1, pp. 873-890. Pergamon.

Wänke H. Wlotzka F. Jagoutz E. and Begemann F. (1970) Composition and structure of metallic iron particles in lunar "fines." *Proc. Apollo 11 Lunar Sci. Conf., Geochim. Cosmochim. Acta*, Suppl. 1, Vol. 1, pp. 931-935. Pergamon.

Winchell H. and Skinner B. J. (1970) Glassy spherules from the lunar regolith returned by Apollo 11 expedition. *Proc. Apollo 11 Lunar Sci. Conf., Geochim. Cosmochim. Acta*, Suppl. 1, Vol. 1, pp. 957-964. Pergamon.

Wosinski J. F. Williams J. P. Korda E. J. Kane W. T. Carrier G. B. and Schreurs J. W. H. (1972) Inclusions and interface relationships between glass and breccia in lunar sample no. 14306.50 (abstract). In *Lunar Science—III* (editor C. Watkins), pp. 811-813. Lunar Science Institute Contr. No. 88.

MORPHOLOGY AND CHEMISTRY OF GLASS SURFACE OF BRECCIA 15015,36. James L. Carter, University of Texas at Dallas, Geosciences Division, Dallas, Texas 75230. Contribution no. 220.

Two types of glassy materials occur in the lunar samples: glass spheres found in the soil and glassy coatings found on rocks. It has been proposed that the craters on the glass spheres occurred mainly in an impact-generated debris cloud (1). The craters on the glassy coating on rocks have been interpreted as arising from micrometeroid bombardment of the glassy surface while in place on the lunar surface (2). The various types of mounds found on the surface of the glass spheres are considered as resulting from both vapor condensation and reduction processes (1,3). The mounds and other similar features on the spheres and the glassy coatings have been compared in an attempt to determine whether the glassy surface coatings were in place on the lunar surface when impacted or if they were produced in an impact-generated debris cloud.

A 62 mm^2 glass surface was coated with gold and examined with a JSM-1 scanning electron microscope and an ARL scanning electron microprobe with an energy dispersive X-ray analyzer. A mosaic of the entire surface was made at 60X (Fig. 1). The glass surface is very frothy or hummocky consisting of a series of depressions and blisters connected by valleys. Many of the blisters are ruptured. Two major areas occur in which large depressions are absent. An enlarged mosaic view of one of the areas (Fig. 2) reveals a wrinkled surface that probably represents a collapse structure. The diameter of the depressions in the wrinkled areas are less than for the overall surface (Fig. 3). This is consistent with a collapse of blisters and continued out-gassing of the host silicate material during cooling.

The glass surface has an assortment of mound types. The larger mounds are primairly concentrated in the valleys with mound size decreasing towards a depression. This suggests that iron migrated from the sides of a depression towards the valleys and due to surface tension mound growth took place there. The larger mounds consist of a central area of metallic iron surrounded by a waist of iron sulfide (Fig. 4). The iron sulfide incompletely wets the mound.

A mosaic of one cluster of mounds is shown by Fig. 4 which is an enlarged view of the central bottom portion of Fig. 1. The surface of the glass area scanned (0.47 mm^2) is covered with mounds over approximately 25 to 30% of its surface with a distribution as shown in Fig. 4. A histogram of the percentage of surface area covered by the various sizes of mounds is shown in Fig. 5. A histogram of the number of mounds versus mound diameter, Fig. 6, reveals that the number of mounds rapidly decreases with an increase in mound diameter. A measurement at 11,500X of 45 square microns (Fig. 7, lower right, Fig. 4) gave approximately 2×10^7 mounds greater than 0.04 microns in diameter and less than 0.5 microns in diameter per square millimeter of the glass surface. A plot of the volume of material in a mound assuming a sphere for the shape of a mound reveals that there are three grouping (Fig. 8).

The less than 4 microns-in-diameter spheres are predominately metallic iron, whereas those larger than 12 microns in diameter are entirely a mixture

of iron sulfide and metallic iron. In the case of dimples for which the mounds are absent the adherance of fragments of iron sulfide to the surface of the dimples (Fig. 4; see also 1,3,5) shows that they were originally mixtures of iron sulfide and metallic iron as suggested by Fig. 8. With the exception of the larger dimples and those near the left margin of the sample, which probably resulted due to the stress of breaking the sample, the dimples are concentrated around a low velocity impact crater.

The mounds do not represent splashes but were grown on the silicate surface. The larger mounds grew at the expense of the smaller mounds. The area immediately surrounding the larger mounds is devoid of smaller mounds. The area of paucity of smaller mounds is elliptical not circular suggesting longitudional migration of molten material on a liquid silicate surface.

The distribution of mounds (Fig. 4) and the mound volume (Fig. 8) suggests that there are different sources for the iron and sulfur. A nucleation site was initiated and the degree of mound growth was a function of the available iron and sulfur at the growth site. A large portion of the metallic iron probably resulted from in situ reduction of the silicate surface (Fig. 7; see also , 3), whereas the sulfur was supplied mainly from an external source such as an impact-generated cloud. Additional iron probably was also supplied by this source.

Another interesting feature of this glass surface is the concentration of irregular or amoeboid-shaped mounds around hills of silicate minerals. An example is seen in the central right portion of Fig. 4. The reason for this type of mound is not known but it may be speculated that in this case there was not sufficient heat to allow the material to coalesce into a sphere by surface tension. It may be that the silicate hill effectively quenched the growth process. This may explain also the paucity of small mounds near the silicate hills.

Possibly the most striking feature of the glass surface is a series of patches ranging from 0.4 to 400 microns in longest dimension that distort the electron beam as it passes over a patch suggesting that they are magnetic. Fig. 7 shows the relationship of this type of structure to other mounds. This is an enlargment of an area just to the right bottom of Fig. 4. The structures appear to be composed of a series of approximately 0.1 to 0.2 micron in diameter spherules and rods. It is thought that this material is metallic iron.

A detailed examination of the mosaic at 60X revealed no hypervelocity craters. 1.07 mm^2 was scanned at 1,150X and again no hypervelocity craters were observed. However, two low velocity craters were noted; one 25 microns in diameter and the other 35 microns in diameter. These data suggest that this glass surface was never exposed to either bombardment by micrometeroids or high velocity projectiles in an impact-generated debris cloud.

References:

1. Carter J. L. and MacGregor I. D., Ap. 11 Lun. Sci. Conf., 247-275, 1970.
2. Hartung J. B. et al., 3 Lun. Sci. Conf., 363-365, 1972.
3. Carter J. L. and McKay D. S., In Press, 1972.
4. Carter J. L. and McKay D. S., 2 Lun. Sci. Conf., 2653-2670, 1971.
5. Carter J. L., 2 Lun. Sci. Conf., 873-892, 1971.

Morphology of Glass Surface

James L. Carter

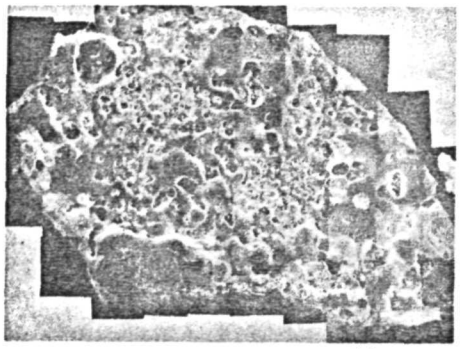

Fig. 1. SEM image, 40X.

Fig. 2. SEM image, central left, Fig. 1, 1,150X.

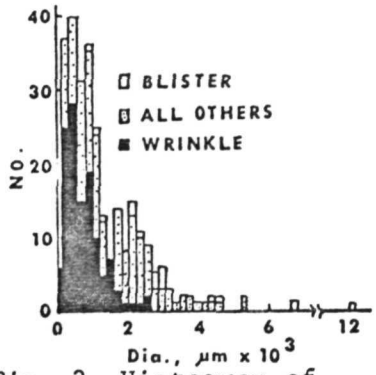

Fig. 3. Histogram of dia. of depressions.

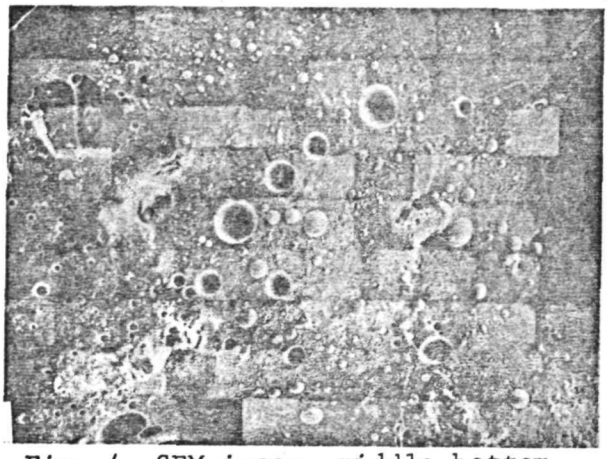

Fig. 4. SEM image, middle bottom of Fig. 1, 1,150X.

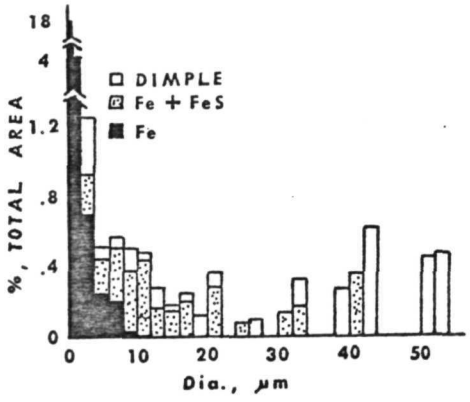

Fig. 5. Histogram of mound dia. versus % of total area.

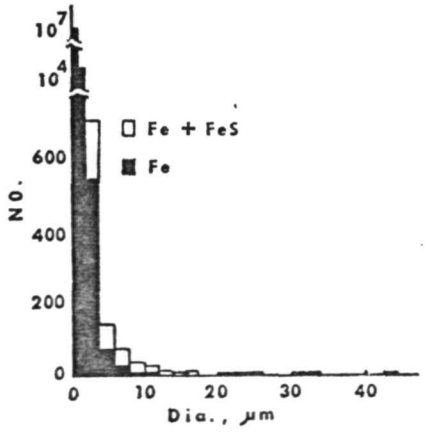

Fig. 6. Histogram of mounds versus dia.

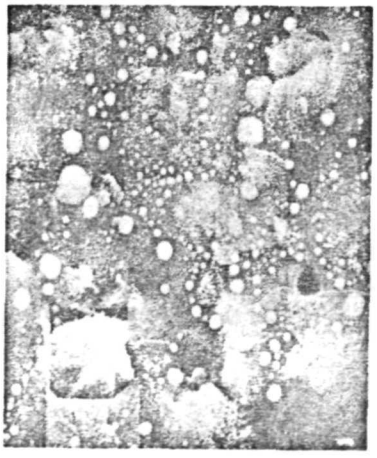

Fig. 7. Enlarged view, lower right of Fig. 4, 11,500X.

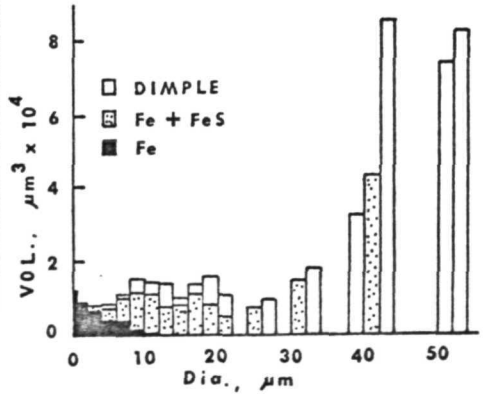

Fig. 8. Histogram of Vol. of mounds versus dia.

CHEMISTRY OF PYROXENES FROM APOLLO SOIL 15501,53. H. C. Jim Taylor and James L. Carter, The University of Texas at Dallas, Geosciences Division, Dallas, Texas 75230. Contribution no. 221.

Delineation of the individual soil and rock types in a composite lunar soil sample can be achieved by electron microprobe studies of the mineral chemistry of a representative set of fragments from a soil sample. This should provide information on the rate of mixing of different soil types and permit identification of rock types not returned as hand specimens. Pyroxenes are ideally suited for this purpose because of their wide range of chemistry and abundance in most lunar types. In soil sample 15501,53, for example, pyroxene fragments are more abundant than plagioclase fragments by approximately 4 to 1.

Partial analyses of 64 pyroxene fragments from the less than 1 mm fraction of the comprehensive sample 15501,53 were obtained using an ARL scanning electron microprobe with an energy dispersive X-ray analyzer. Analyses for Si, Fe, Mg, Ca, Ti, and Al were made on fragments within the 75 to 150 micron fraction. These occurred primarily as individual grains, but also occurred as components within microcrystalline fragments, agglutinates, and microbreccias.

The pyroxene fragments analyzed cover a wide area of the pyroxene quadrilateral (Fig. 1), ranging from augites, subcalcic augites, and low-calcium, magnesium pyroxenes to ferroaugites, subcalcic ferroaugites, and pyroxferroites. No one type is dominant but the distribution is not random. Plots of the chemical components clarify the possible trends. For example, the plot of Al/Si versus Fe/Mg (Fig. 2) suggests two distinct trends; one of increasing alumina enrichment similar to the early trend of rock 15499 (1). The other is a very distinct trend of extreme iron enrichment which suggests the presence of a genetically separate group of pyroxene fragments in this soil sample. The plot of Ti versus Al (Fig. 3) is consistent with the conclusion that more than one genetic unit is represented by these pyroxenes.

The mixing of genetically unrelated fragments from different lunar localities could result in the observed variation of pyroxene chemistry. Such a process, based upon the efficiency of meteoritic impacts into the lunar regolith as a transport and mixing mechanism, may explain the extreme variations noted. The trends observed are consistent with the mixing of soils from the rill area and the ray trending through the LM site (2). Alternatively, a wide range of melt compositions combined with the partitioning of chemical components between the melt and crystalline phases could explain the variation in the observed pyroxene chemistry.

References

(1) Bence, A.E., Proc. 7 Nat. Conf. EPA, EPASA, 51A-51C, 1972.
(2) Apollo 15 Prel. Exam. Team, Sci. 175, 363-375, 1972.

CHEMISTRY OF PYROXENES

H.C. Jim Taylor

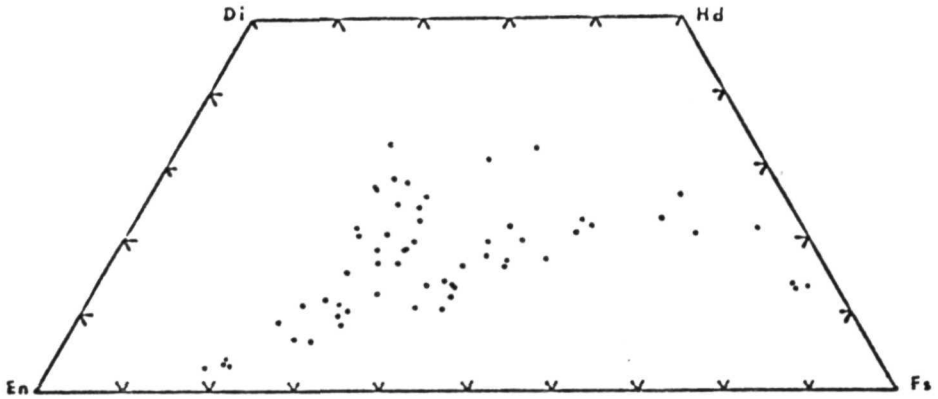

Fig. 1. Composition of pyroxenes.

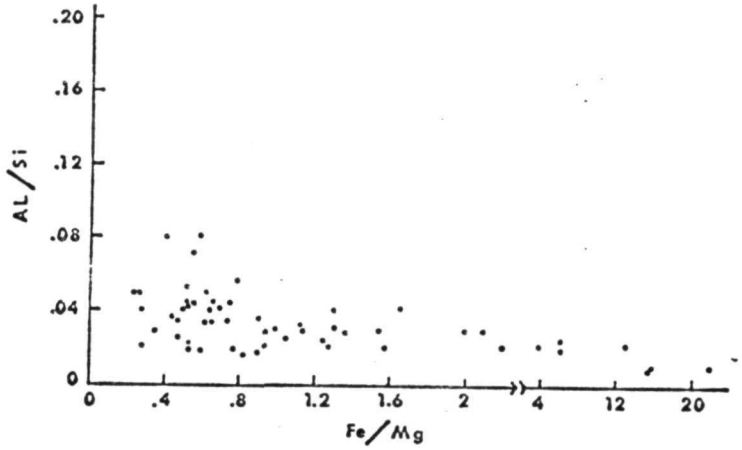

Fig. 2. Al/Si vs. Fe/Mg (atomic proportions, O = 6).

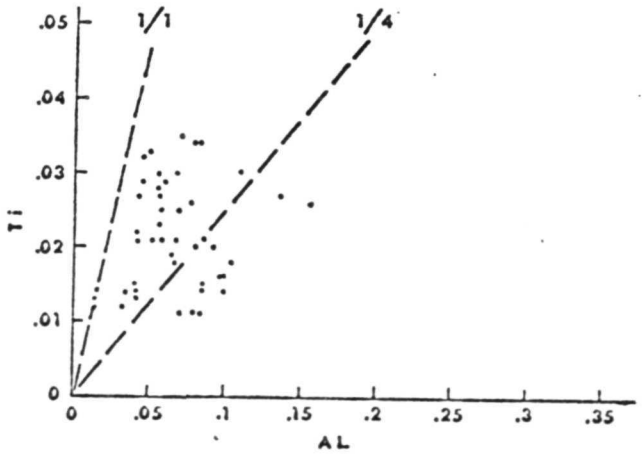

Fig. 3. Ti vs. Al (atomic proportions, O = 6).

American Geophysical Union
1707 L Street, N.W.
Washington, D.C. 20036 U.S.A.

Abstract form for FALL ANNUAL, 1972 Meeting

Submitted to Section (Sub-Section) of Vol. Geochem. Petrol.

Surface Morphology and Chemistry of Rock 15015,36. A 62 mm^2 glass surface was examined with a JSM-1 scanning electron microscope and an ARL scanning electron microprobe with an energy dispersive x-ray analyzer. A 60X (spatial resolution of 8 microns) mosaic of the surface was made. The frothy glass surface consists of a series of depressions and blisters connected by valleys. No hypervelocity-type craters were observed at 60X. 1.07 mm^2 was scanned at 1,150X (spatial resolution of 0.4 microns) and again no hypervelocity-type craters were seen. These data suggest that the glass surface was exposed neither to bombardment by micrometeroids nor relatively high velocity projectiles in an impact-generated debris cloud. The glass surface has an assortment of mound types. The mounds greater than 12 microns in diameter consist of a central area of metallic iron surrounded by a waist of iron sulfide and are primairly concentrated in the valleys with mound size decreasing towards a depression. The mounds less than 4 microns in diameter are mainly metallic iron. The distribution of mound types and the relationship of mound volume to mound diameter suggests that there are different sources for iron and sulfur. A large portion of the metallic iron probably resulted from in situ reduction of the molten silicate surface, whereas the sulfur was supplied mainly from an external source such as an impact-generated vapor cloud.

James L. Carter
Inst. for Geol. Sciences
The Univ. of Texas at
Dallas, P.O. Box 30365,
Dallas, Texas. 75230.

A Comparison of Pyroxenes from Lunar Soil Samples 15411,46 and 15501,53. Pyroxene fragments from the 75 to 150 micron fraction of the two comprehensive samples were analyzed by electron microprobe techniques for Si, Fe, Mg, Ca, Ti, and Al. They occur as individual grains and as components in microcrystalline fragments, microbreccias, and agglutinates. No preferred compositions were observed in the single crystals versus the other occurrences. Soil sample 15411,46 (Stat. 7) contains bronzites, magnesium pigeonites, subcalcic augites, augites, ferroaugites, and subcalcic ferroaugites in an abundance ratio of about 3:3:1:1:1:1. Soil sample 15501,53 (Stat. 9) contains bronzites, magnesium pigeonites, intermediate pigeonites, subcalcic augites, augites, ferroaugites, subcalcic ferroaugites, and pyroxferroites in an abundance ratio of about 1:3:2:3:2:1:4:1. Pyroxenes from the Stat. 9 soil are indicative of a continuous basaltic fractionation trend towards extreme iron enrichment, as opposed to the Stat. 7 soil which contains a distinctive abundance of Mg-rich pyroxenes and lacks pyroxene compositions denoting continuous, as well as extreme, iron enrichment. These data indicate that thorough mixing of soil components has not occurred throughout the Apollo 15 sampling area, and that limitations must be applied to models involving mixing mechanisms and soil transport over long distances on the lunar surface.

H. C. Jim Taylor
James L. Carter
Inst. for Geol. Science
The Univ. of Texas at
Dallas, Box 30365,
Dallas, Tex. 75230